Catalysis Letters 18 (1993) 373–389

Reactions of methylbutynol on alkali-exchanged zeolites. A Lewis acid–base selectivity study

M. Huang and S. Kaliaguine[1]

Département de Génie Chimique et CERPIC, Université Laval, Québec, Canada

Received 12 December 1992; accepted 1 March 1993

Alkali-exchanged zeolites have both Lewis acid and Lewis base centres. They provide an easy way to tune up the relative strengths of these two sites by controlling Si/Al ratio and electropositivity of the counter cation. These effects can be monitored both by FTIR and N_{1s} XPS of chemisorbed pyrrole. A systematic study of the relationship between acid–base properties and the reactions of methylbutynol (MBOH) was performed over these alkali-exchanged zeolites. The results show that the Lewis base centres catalyze the cleavage reaction of MBOH, which produces acetone and acetylene, while the strong Lewis acid centres catalyze the dehydration of MBOH to 3-methyl-3-buten-1-yne (MBYNE). The strong basicity of alkali-exchanged X zeolites produces almost 100% selectivity to acetone and acetylene, whereas the strong Lewis acidity of alkali-exchanged ZSM-5 zeolites results in a high selectivity to MBYNE. Compared with the catalytic results over H-ZSM-5 zeolites, it is further concluded that the catalytic conversion of MBOH to 3-methyl-3-butene-2-one (MIPK) requires the presence of not Lewis acid but strong Brønsted acid sites. The reactions of MBOH over acid–base catalysts are considered as standard reactions for the characterization of acid and base centres. A correlation between these reactions and the FTIR, and XPS of pyrrole data will be discussed. The deactivation mechanism during MBOH conversion over alkali-exchanged zeolites is further discussed.

Keywords: Methylbutynol reactions; alkali-zeolites; Lewis acid–base

1. Introduction

The acidity and basicity of zeolites are important in determining the catalytic activity and selectivity for zeolite-catalyzed reactions. Recently, we suggested a model for the adsorption of pyrrole on Lewis basic and the conjugate Lewis acid sites in alkali-exchanged zeolites [1,2]. The local environment of these sites was emphasized in determining zeolite basicity [3,4]. It was further demonstrated that both the FTIR NH stretching frequency [3] and N_{1s} XPS [4] of chemisorbed pyrrole

---

[1] To whom correspondence should be addressed.

can be used to characterize zeolite basicity. In general, the stronger the basic site, the lower the NH stretching frequency and also the N_{1s} binding energy. The results revealed that the zeolite basic strength decreases with an increase in Si/Al ratio of the zeolite framework, and increases when the electropositivity of counter alkali cations was raised. The counter cations should be regarded as Lewis acid sites and their acid strength increases with Si/Al ratio and decreases with electropositivity. Pyrrole may also interact with these Lewis acid sites and produces some characteristic bands in the ring-stretching region of infrared spectra.

In the present work, in order to complement the above knowledge, the reactions of methylbutynol were performed over alkali-exchanged zeolites. The reactions of methylbutynol were first recommended by Lauron-Pernot et al. [5] to characterize the acid–base properties of a series of metal oxides. The basic centres catalyze the cleavage reaction of MBOH, which produces acetone and acetylene, while the acid centres catalyze the dehydration of MBOH to 3-methyl-3-buten-1-yne (MBYNE) or the intermolecular rearrangement to produce 3-methyl-2-butenal (PRENAL). The production of 3-methyl-3-butene-2-one (MIPK) and 3-hydroxy-3-methyl-2-butanone (HMB) from MBOH was also observed in the presence of amphoteric sites. However, as pointed out by these authors, the kind of the acid–base sites responsible for the different products remains unresolved and further work is necessary. Thus the reactions of MBOH are also considered as standard reactions here for the characterization of acid and base centres. A correlation between these reaction results and the previously observed FTIR, and XPS of chemisorbed pyrrole data will be shown, and the effect of the nature of solid base and acid centres on the product selectivity will be further discussed.

2. Experimental

Various alkali-cation exchanged faujasite, mordenite and ZSM-5 zeolites were prepared from the sodium forms contacted with the corresponding chloride solution, while the alkali-cation exchanged L zeolites were prepared from the potassium form. The exchange temperature was maintained at 70–80°C and the time for a single exchange was around 24 h. In most cases up to three successive exchanges had to be performed in order to obtain high exchange levels. Details of the preparation of H-ZSM-5 have been previously described [6]. The bulk chemical composition of zeolites was established by atomic absorption using a Perkin-Elmer (model 1100B) spectrometer. Table 1 lists the unit-cell compositions of all zeolite samples used in this work. The results revealed that the exchange level of alkali cations is 100% for ZSM-5 samples but less than 100% for other zeolites [3]. For comparison, two kinds of Brønsted bases (containing OH^- groups) were also tested by MBOH reaction. The first was mounted bases, which were prepared by impregnation of 5 g SiO_2 with 10 ml of a solution containing 1.2 g of KOH, followed by evaporation

Table 1
Unit-cell composition of zeolite samples

LiX	$Li_{54.3}Na_{31.1}(AlO_2)_{85.4}(SiO_2)_{106.6}$
NaX	$Na_{85.4}(AlO_2)_{85.4}(SiO_2)_{106.6}$
KX	$K_{48.3}Na_{37.1}(AlO_2)_{85.4}(SiO_2)_{106.6}$
RbX	$Rb_{37.7}Na_{47.7}(AlO_2)_{85.4}(SiO_2)_{106.6}$
CsX	$Cs_{28.8}Na_{56.6}(AlO_2)_{85.4}(SiO_2)_{106.6}$
NaA	$Na_{11.9}(AlO_2)_{11.9}(SiO_2)_{12.1}$
NaY	$Na_{54.5}(AlO_2)_{54.5}(SiO_2)_{137.5}$
NaL	$Na_{8.0}K_{0.9}(AlO_2)_{8.9}(SiO_2)_{27.1}$
NaM (mordenite)	$Na_{7.9}(AlO_2)_{7.9}(SiO_2)_{40.1}$
Li-ZSM-5	$Li_{2.3}(AlO_2)_{2.3}(SiO_2)_{93.7}$
Na-ZSM-5	$Na_{2.3}(AlO_2)_{2.3}(SiO_2)_{93.7}$
K-ZSM-5	$K_{2.3}(AlO_2)_{2.3}(SiO_2)_{93.7}$
Rb-ZSM-5	$Rb_{2.3}(AlO_2)_{2.3}(SiO_2)_{93.7}$
Cs-ZSM-5	$Cs_{2.3}(AlO_2)_{2.3}(SiO_2)_{93.7}$
H-ZSM-5	$H_{2.4}(AlO_2)_{2.4}(SiO_2)_{93.6}$

at room temperature and drying at 200°C for 1 h. The other base was commercial $Ca(OH)_2$.

The MBOH reactions were carried out in a continuous flow reactor operated at atmospheric pressure. 0.05 g of catalyst was packed in a reactor placed in a vertical furnace, and then heated under an Ar stream up to 400°C. The temperature of reactor was then decreased to 180°C in the Ar atmosphere, and the MBOH vapour at 60°C (~ 160 Torr) was introduced using Ar as the vector gas with a W/F of 0.2 g h mol^{-1}. The activation procedure was different for Brønsted bases. Since the bases may decompose at high temperature, these samples were just swept using Ar when the temperature of reactor was raised from room temperature to 180°C. Then the MBOH vapour at 60°C was also introduced using Ar as the vector gas. The effluent gas from the reaction tube was analyzed using a SIGMA 115 gas chromatographic system, and a 3 m Porapack Q column. The catalytic results are expressed in terms of conversion and molar distribution of the products. C_i is the molar concentration of compound i in the vapour phase and $(C_{\mathrm{MBOH}})^0$ the initial molar concentration of MBOH. Since the reactions were carried out at atmospheric pressure and the molar flow of Ar was much larger than that of MBOH in the feed (about 5 : 1), the change in volume during the reactions can be omitted. Then conversion is defined as follows:

$$\mathrm{conv}\% = [(C_{\mathrm{MBOH}})^0 - C_{\mathrm{MBOH}})]/(C_{\mathrm{MBOH}})^0 \,. \tag{1}$$

The total resulting products concentration is defined as: $\sum \alpha_i C_i$, with $\alpha_i = 1$ for all products, except for acetone and acetylene for which, in order to normalize conversion to 100%, $\alpha_i = 0.5$. The molar distribution for product i can be defined as

$$S_i = \alpha_i C_i / \sum \alpha_i C_i \,. \tag{2}$$

In most experiments $C_{\mathrm{MBOH}} + \sum \beta_i C_i$ is usually different from $(C_{\mathrm{MBOH}})^0$, where β_i is the ratio of carbon number in product i to that in MBOH. The carbon unbalance is therefore defined as

$$\left[C_{\mathrm{MBOH}} + \sum \beta_i C_i - (C_{\mathrm{MBOH}})^0\right] / (C_{\mathrm{MBOH}})^0 . \tag{3}$$

The initial activity of catalysts was monitored by the results obtained after 5 min of reaction, while the results after 55 min were further recorded in order to compare the deactivation behaviour.

Zeolite samples for infrared experiments were pressed into self-supported wafers of roughly 10 mg. These wafers were mounted in a pyrex cell fitted with calcium fluoride windows and then connected to the vacuum system. Before infrared measurement the samples were degassed at 400°C overnight ($p = 10^{-5}$ Torr). All the spectra were recorded with a 2 cm^{-1} resolution, using a Digilab FTS-60 spectrometer.

3. Results

3.1. CATALYTIC REACTIONS OF METHYLBUTYNOL (MBOH)

Table 2 shows the results obtained after MBOH reaction over alkali-exchanged X zeolites, MgO and the Brønsted base samples. Among zeolite samples, the initial conversion after 5 min increased with the counter cations in the order Li < Na $\approx$ K < Rb < Cs. The activities declined rapidly with reaction time for Li-, Na-, K- and Rb-exchanged X zeolites but more slowly for Cs-exchanged X zeolite. The carbon unbalance was important for all the zeolite samples. After 5 min of reaction the sum of product molar carbon flow rates was less than the one for con-

Table 2
MOBH reaction over alkali-exchanged X zeolites and MgO

	Sample							
	LiX	NaX	KX	RbX	CsX	MgO	KOH/SiO_2	$Ca(OH)_2$
reaction time = 5 min								
conv. (%)	68.3	72.8	72.4	85.8	88.0	96.7	85.0	96.7
product distribution (%)								
C_2H_2	11.3	57.4	50.0	46.7	66.1	51.3	45.9	51.5
C_3H_6O[a]	88.7	42.6	50.0	53.3	33.9	48.7	54.1	48.5
C unbalance (%)	−25	−35	−32	−47	−39	~0	−76	−58
reaction time = 55 min								
conv. (%)	5.6	58.8	34.1	37.6	69.2	95.7	44.2	91.6
product distribution (%)								
C_2H_2	6.7	50.5	45.7	43.9	46.5	50.0	46.8	51.6
C_3H_6O[a]	93.3	49.5	54.3	56.1	53.5	50.0	53.2	48.4
C unbalance (%)	34	35	35	32	19	23	−40	−32

[a] Acetone.

verted MBOH, while this sum became larger than the converted MBOH after 55 min of reaction. The only products detected over these samples were acetone and acetylene, and the distribution of every product was nearly the same for all samples except Li-X, where the distribution of acetylene was much smaller than that of acetone. The highest conversion in table 2 is found in the case of MgO. Moreover, the deactivation during the same reaction time over MgO is negligible. The Brønsted bases also show quite high conversion, but the deactivation becomes more serious. It is interesting to find that the only products detected over MgO, KOH/SiO_2 and $Ca(OH)_2$ were also acetone and acetylene. Since MgO is a typical Lewis base, then one conclusion is that there is no difference in product selectivity of MBOH reaction between Lewis and Brønsted bases. In other words, the MBOH standard reaction is not sensitive to the nature of solid bases.

The same reaction was also performed over a series of Na-exchanged zeolites and the results are listed in table 3. Clearly, the activity decreased as the Si/Al ratio increased from zeolite A to mordenite, but it was dramatically enhanced over Na-ZSM-5 zeolite. The products detected over A, X and Y zeolites were still acetone and acetylene, but MBYNE appeared as another reaction product over L zeolite, and it became the dominant product over ZSM-5 zeolite (96% distribution). A tiny amount of MIPK and PRENAL were also detected over L, mordenite and ZSM-5 samples. The completely different product distribution and also the enhanced

Table 3
MBOH reaction over Na-exchanged zeolites

	Zeolite					
	A	X	Y	L	mordenite	ZSM-5
reaction time = 5 min						
conv. (%)	83.6	72.8	46.8	37.4	22.5	82.5
product distribution (%)						
C_2H_2	49.7	57.4	63.5	50.3	48.8	3.2
$C_3H_6O^a$	50.3	42.6	36.5	41.7	50.5	~0
MBYNE	0	0	0	6.5	~0	95.9
PRENAL	0	0	0	0.2	0.4	0.1
MIPK	0	0	0	0.2	0.3	0.8
C unbalance (%)	−20	−35	−25	−32	−16	−52
reaction time = 55 min						
conv. (%)	77.1	58.8	31.3	5.3	4.6	37.6
product distribution (%)						
C_2H_2	48.4	50.5	46.5	38.0	49.0	2.3
$C_3H_6O^a$	51.6	49.5	53.5	43.0	51.0	~0
MBYNE	0	0	0	17.7	~0	84.2
PRENAL	0	0	0	0.4	~0	9.2
MIPK	0	0	0	0.4	~0	4.3
C unbalance (%)	8	35	−26	~0	~0	−10

[a] Acetone.

activity revealed a completely different reaction route over Na-ZSM-5 from that over alkali-exchanged X zeolites. It was further found that after 55 min of reaction the deactivation changed with Si/Al ratio of zeolites in the same order, the larger this ratio, the deeper the decline in activity from zeolite A to mordenite. The carbon unbalance was still serious over these samples.

Table 4 shows catalytic results obtained over ZSM-5 samples. In the beginning, after 5 min of reaction the highest conversion was found in the case of H-ZSM-5, while the conversions over the other ZSM-5 samples are at similar levels. The product distribution of acetylene is less than 10% over H-, Li-, Na-, K- and Rb-exchanged ZSM-5 samples, but still quite high over Cs-ZSM-5 sample. However, no detectable amount of acetone was found in all cases. The MBYNE was certainly the dominant product over alkali-exchanged ZSM-5 zeolites, tiny amounts of MIPK and PRENAL were also detected over these samples. After 55 min of reaction the activity was reduced while the product distributions of MIPK and PRENAL increased. The situation of H-ZSM-5 was different. In the beginning, the main products are MBYNE and MIPK with nearly the same product distribution (49 and 45%). However, when the activity decreased the distribution of MIPK dramatically diminished while the distributions of MBYNE and PRENAL increased remarkably.

3.2. FTIR RESULTS

After dehydration at 400°C MBOH vapour was introduced at room tempera-

Table 4
MBOH reaction over ZSM-5 zeolites

	Cation					
	Li	Na	K	Rb	Cs	H
reaction time = 5 min						
conv. (%)	67.9	82.5	74.0	75.5	72. 3	99.1
product distribution (%)						
C_2H_2	7.9	3.2	6.7	3.5	21.1	1.4
MBYNE	90.3	95.9	93.1	96.5	78.8	49.6
PRENAL	0.5	0.1	~0	~0	~0	3.9
MIPK	1.3	0.8	0.2	~0	~0	45.1
C unbalance (%)	−48	−52	−40	−56	−38	−36
reaction time = 55 min						
conv. (%)	9.0	37.6	39.7	31.2	24.0	80.8
product distribution (%)						
C_2H_2	12.1	2.3	3.0	3.1	9.9	0.4
MBYNE	80.1	84.2	92.4	95.5	85.9	73.1
PRENAL	2.9	9.2	3.6	0.4	3.8	22.9
MIPK	4.9	4.3	1.0	1.0	0.4	3.6
C unbalance (%)	~0	−10	−8	−23	4	6

ture into the infrared cell. The representative changes in infrared spectra observed on the Li-X sample upon adsorption of MBOH are shown in fig. 1. Compared with gas phase the adsorbed MBOH displayed a very broad band around 3300–3400 cm^{-1} with a relatively sharp peak at 3283 cm^{-1}. Meanwhile bands were also detected at 2988, 2940, 1465, 1380 and 1370 cm^{-1}, which can also be found in the gas phase spectrum [7] of MBOH with slightly different wavenumbers. The appearance of broad band around 3300–3400 cm^{-1} usually suggests the hydrogen bonding between OH groups or a polymerized adsorption form of MBOH molecules [8]. The relatively sharp peak at 3283 cm^{-1} could possibly be the weakened C≡C band, which is located at 3328 cm^{-1} for gaseous MBOH [7]. After heating and evacuation at 180°C a dramatic change was found in the spectrum. A strong band located at 1708 cm^{-1} appeared accompanied by the bands at 2920, 1675, 1470 (very weak), 1423 and 1372 (increased compared with the original 1370 cm^{-1}) cm^{-1}, while the bands belonging to the adsorbed MBOH still remained with reduced intensities. Since acetone was detected by GC after reaction, the 1708 cm^{-1} band is assigned to the C=O stretching vibration (referred as $\nu 1$ or main C=O band) of adsorbed ac-etone. However, the 1423 cm^{-1} belongs to the CH_2–CO bending frequency [8] and the 2920 cm^{-1} belongs to the ν_{as} of CH_2 group [8]. The ν_s band of CH_2 group should be weaker [8] and may therefore correspond to a very weak band around 2850 cm^{-1}. The aldol condensation of acetone to form diacetone alcohol

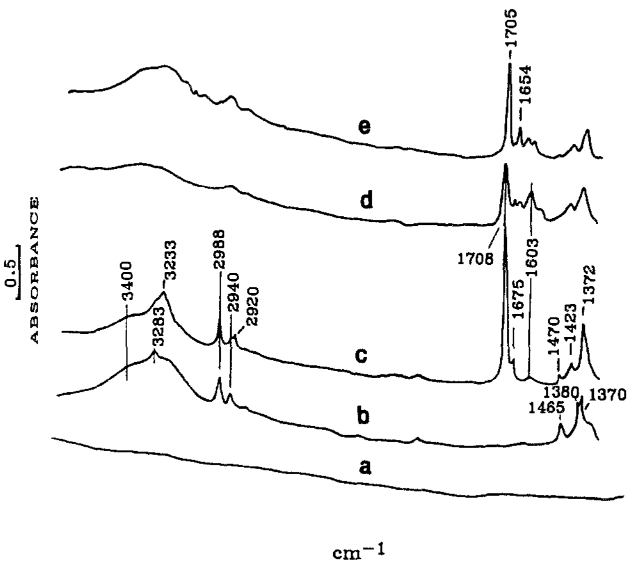

Fig. 1. IR spectra of (a) LiX, after dehydration at 400°C overnight; (b) LiX, after adsorption of MBOH at room temperature for 5 min, followed by evacuation at room temperature for 1 h; (c) LiX, after heating at 180°C for 30 min and further evacuation at 180°C for 1 h; (d) LiX, after further evacuation at 180°C overnight; (e) NaX, after adsorption of MBOH at room temperature and evacuation at 180°C overnight.

is a well known reaction [9] catalyzed by basic catalysts. Thus the presence of CH_2 groups may indicate the condensation of adsorbed acetone. The frequency of another weak band at 1675 cm^{-1} is still in the C=O stretching region [8], which means another form of adsorbed acetone with a weakened C=O bond (referred as $\nu2$ or second C=O band). The 1470 cm^{-1} is consistent with the phenyl nucleus vibration frequency of benzene adsorbed on zeolites [10,11]. Since acetylene was formed with a relatively small product selectivity over Li-X, the formation of benzene means the cyclotrimerization of acetylene over Li-X zeolite. However, the concentration of adsorbed benzene after desorption at 180°C must be very low, since the 1470 cm^{-1} band, which should be the strongest among adsorbed benzene bands [10,11], is very weak and also the other benzene bands around 3000 cm^{-1} cannot be clearly detected. This phenomenon is consistent with literature results, for example, 100°C was enough to remove the adsorbed benzene on NiY zeolite [11]. On the other hand, the benzene bands cannot be detected in the cases of other samples. After evacuation at 180°C for a longer time the main change in the IR spectrum over the LiX sample is the increase of 1603 cm^{-1} band, which could mean the formation of carbonaceous materials [12] with a structure similar to triene [8]. However, the main change after long time evacuation at 180°C for other X zeolites is the appearance of a C=C band located at 1654 cm^{-1} [9]. As an example, a representative spectrum of NaX is shown in fig. 1e. A reasonable explanation for this change may be the further dehydration of adsorbed diacetone alcohol.

Fig. 2 shows the IR spectra of all alkali exchanged X zeolites after adsorption of MBOH and further evacuation at 180°C . The 1420 and 2920 cm^{-1} bands were also found in all the spectra of these samples. Similarly, combined with the broad band around 3300 cm^{-1} and the 1700 cm^{-1} C=O band, these bands suggest the formation of diacetone alcohol. It is further noted that the intensity of the C=O band is reduced from Li to Cs. Another C=O band with lower frequency around 1670 cm^{-1} ($\nu2$) was detected in the cases of LiX, NaX and KX, but it was not observed in the cases of RbX and CsX. Fig. 3 shows the IR spectra of all Na-exchanged zeolites and MgO after adsorption of MBOH and further evacuation at 180°C . The C=O band observed on Na-A zeolite possesses the lowest frequency (1666 cm^{-1}) and weaker intensity, however, this band appeared immediately after adsorption of MBOH even at room temperature. In contrast, the C=O frequencies observed on Y, L, mordenite (very weak) and ZSM-5 samples are higher (1713 cm^{-1}) than that on X zeolites, meanwhile, the band around 1420 cm^{-1} became very weak for Y and L zeolites and absent for A, mordenite and ZSM-5 zeolite. The second C=O band ($\nu2$) was also detected for Y zeolite (1690 cm^{-1}). The situation of H-ZSM-5 and MgO is quite different. The former has a band located at 1615 cm^{-1} and a shoulder at 1605 cm^{-1}, while the original OH band at 3612 cm^{-1} disappeared. Since the MIPK was detected just over this sample, then the 1615 cm^{-1} is still assigned to the C=O frequency of adsorbed MIPK, which formed H-bonding with zeolite protons or just the intramolecular H-bonding [8]. The MgO does not

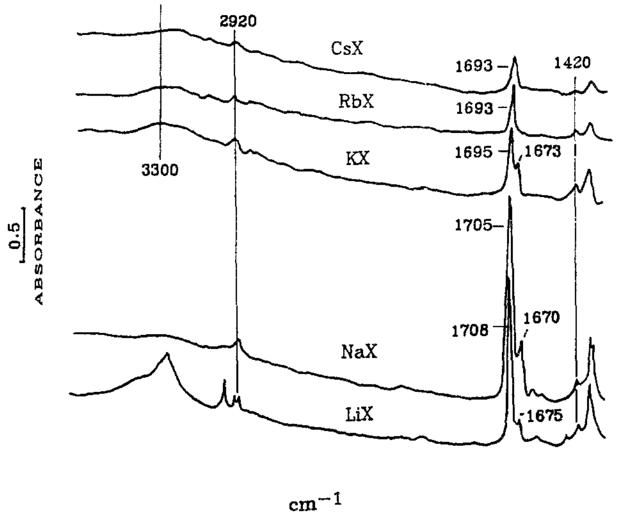

Fig. 2. IR spectra of MBOH adsorbed on alkali-exchanged X zeolites. After heating at 180°C for 30 min and further evacuation for 1 h.

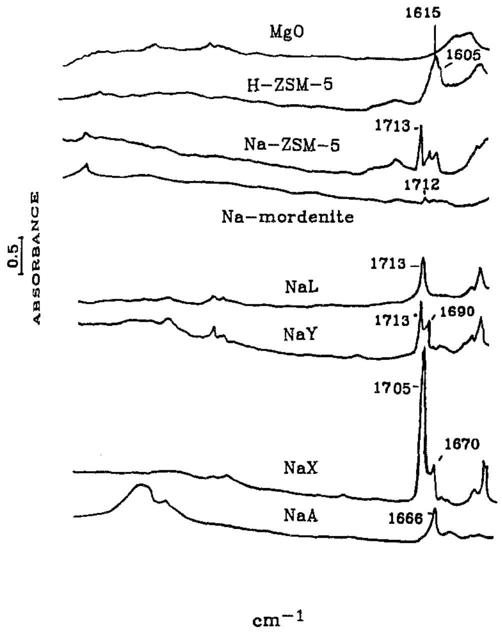

Fig. 3. IR spectra of MBOH adsorbed on Na-exchanged zeolites, H-ZSM-5 and MgO. After heating at 180°C for 30 min and further evacuation for 1 h.

hold any C=O band after desorption at 180°C, through the bands belonging to the residual adsorbed MBOH can be still detected.

4. Discussion

4.1. LEWIS ACID–BASE SELECTIVITY

Table 2 shows that the only products of MBOH reaction over alkali-exchanged X zeolites are acetone and acetylene, which should be produced by basic catalysts. This result is totally expected, since the previous infrared [3] and XPS [4] investigation revealed the presence of strong Lewis basic sites over this samples. The strength of basic sites can be characterized by both the infrared NH stretching frequency and the N_{1s} binding energy of adsorbed pyrrole. Fig. 4 shows that both of these two parameters are well correlated with the MBOH conversion. Thus the activity in MBOH reaction can be taken as another standard test of the base strength. However, the catalytic conversion over MgO is much higher than what can be expected from the basicity, since its high NH stretching frequency indicated a relatively lower base strength than that of alkali-exchanged X zeolites. The reason is apparently due to the serious deactivation over X zeolites, which will be discussed later. A mechanism similar to that suggested by Lauron-Pernot et al. [5] is then drawn in scheme 1 for the reaction over Lewis basic sites, however, the role of the conjugate Lewis acid site is also pictured in this scheme.

The results in table 3 revealed the change in catalytic activity and product distribution with the Si/Al ratio. Since acetone and acetylene are produced over basic sites, while MBYNE and PRENAL are produced over acid sites, then the yield of

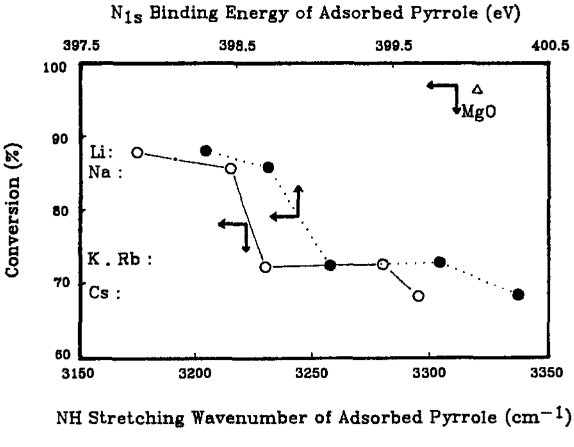

Fig. 4. Relationship between MBOH reaction activity and the FTIR, XPS data of chemisorbed pyrrole over X zeolites.

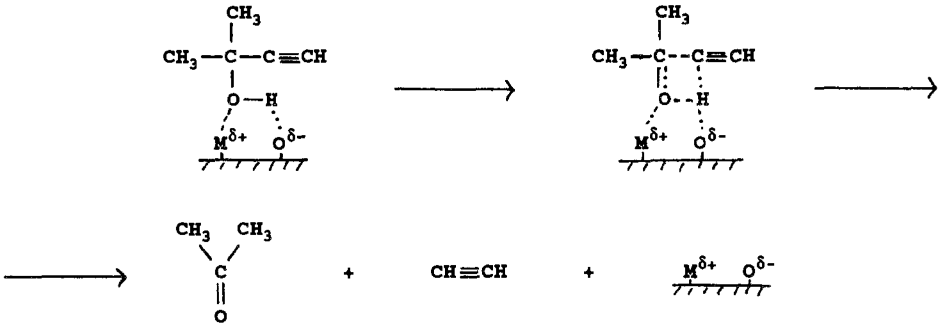

Scheme 1.

acetone plus acetylene can be roughly taken as a measurement of basicity and the yield of MBYNE plus PRENAL as one of acidity. Using these data, fig. 5 shows that the basicity monotonously decreases while the acidity increases with the Si/Al ratio. This is also consistent with the infrared observation [3], which revealed that the strong NH stretching bands for NaX (3280 cm^{-1}) and NaY (3390 cm^{-1}) correspond to the presence of Lewis basic sites, while there are no detectable bands belonging to Lewis acid sites over NaX and NaY samples. On the other hand, infrared spectra [1,3] also show that the main NH stretching bands for NaL (3406 cm^{-1}), NaM (3420 cm^{-1}) and Na-ZSM-5 (3465 cm^{-1}) correspond to the presence of Lewis acid sites, while the bands responsible for the Lewis base sites are very weak over these samples. Here, only over NaL, NaM and Na-ZSM-5 samples

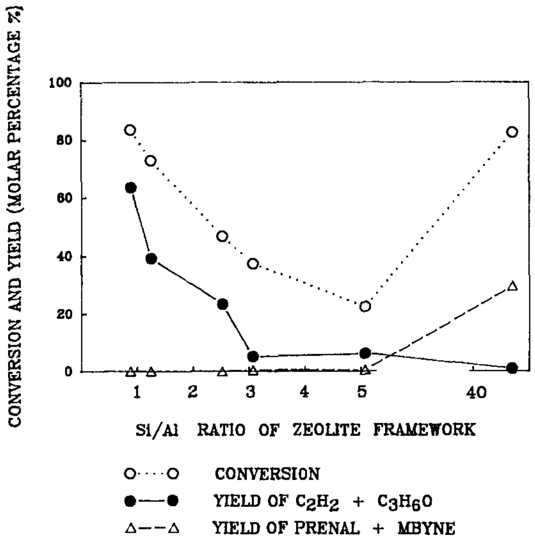

Fig. 5. Conversion and product yield after 5 min of MBOH reaction at 180°C over Na-exchanged zeolites.

which possess strong Lewis acid sites, were MBYNE and PRENAL detected. It is further noticed that the amount of PRENAL is always a small portion of the products. Particularly, over all alkali-exchanged ZSM-5 zeolites (table 4), which possess the highest Si/Al ratio and hence the highest Lewis acidity, the main product is MBYNE (more than 90% for Li, Na, K, Rb-ZSM-5 and 78% for Cs-ZSM-5). In addition to pyrrole adsorption, infrared investigation using pyridine as probe molecule was also performed [13] over these samples. The results confirm that there are no Brønsted acid sites but pyridine species associated with Lewis acid sites – the alkali cations. This observation is consistent with pyridine TPD results carried out by Haber and coworkers [14]. These authors did not find Brønsted but Lewis acid sites over a series of alkali-exchanged ZSM-5 samples. Therefore it is safe to conclude that the main role of Lewis acid sites during MBOH reactions is the dehydration of MBOH to form MBYNE. Scheme 2 proposes a mechanism for MBOH reaction over Lewis acid sites.

Like in scheme 1, both Lewis acid and Lewis base sites take part in reaction scheme 2. However, since the basicity of alkali-exchanged ZSM-5 is very weak, its role in scheme 2 may not be important. For example, one hydrogen atom of CH_3 group could be directly captured by the OH group, which is activated by the Lewis acid site. In any cases the different reaction products between scheme 1 and 2 are mainly caused by the different acid and base strength. The O–H bond is stronger than the C–H bond, thus only the strong basic site can abstract a hydrogen atom from the OH group, finally resulting in the formation of acetone and acetylene. On the other hand, compared with scheme 1, the complete rupture of the C–O bond in scheme 2 requires stronger attractive power of cations, i.e., strong Lewis acidity. That could be why the MBYNE cannot be formed over alkali-exchanged A, X and Y zeolites, even though the stronger basicity of these samples in favour of the rupture of C–H bond.

Another point from fig. 5 is that controlling the Si/Al ratio provides another way to tune up the relative strengths of basic and acid sites. The dramatic increase of both conversion and MBYNE yield over Na-ZSM-5 zeolite means a dramatic

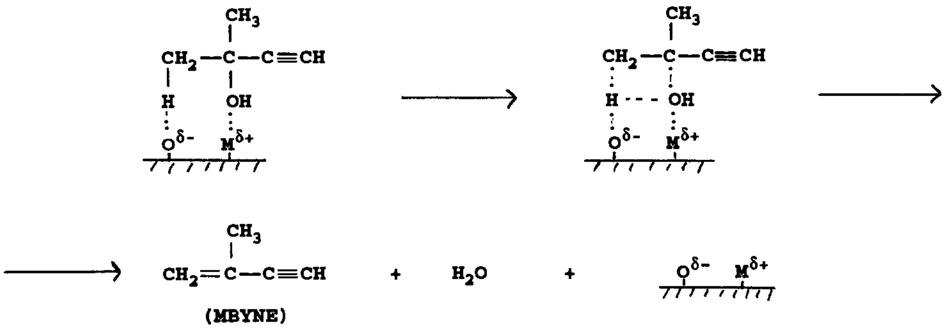

Scheme 2.

increase of Lewis acidity. The reason for the strong Brønsted acidity of H-ZSM-5 has been discussed by many authors [15,16]. In general, the high Si/Al ratio will result in a lower electron density on the framework oxygens [15], thus the protons will be more loosely bonded to these oxygens and therefore the acid strength increases. A similar explanation could be also suitable for the strong Lewis acidity observed here. The high Si/Al ratio and lower electron density on the framework oxygens will correspond to weak bonding between framework oxygens and the extraframework alkali cations, and finally results in a lower electron density over these alkali cations. Therefore, the electron pair acceptance power of these cations increases, that is, the Lewis acidity increases.

By contrast to alkali-exchanged ZSM-5 samples, as high as 45% of products was detected as MIPK over H-ZSM-5 sample in the beginning of reaction. It was suggested [5] that the formation of MIPK requires the presence of both acid and basic sites. Weak basic sites exist on both H- and alkali-exchanged ZSM-5 samples as revealed by the detection of acetylene. Thus the main difference between these two catalysts is the nature of acid sites. In other words, the presence of Brønsted acid sites is required for the formation of MIPK. A simple mechanism including the formation of carbenium intermediates is suggested in scheme 3.

Clearly, according to this mechanism, the formation of MIPK does not require the presence of amphoteric sites but of Brønsted sites only. Additional evidence to support this mechanism is the fact that MIPK was also produced in the MBOH reaction in concentrated sulfuric acid [17]. However, similar to the conclusion of Lauron-Pernot et al. [5], we suggest that the acid sites involved in MIPK formation are strong Brønsted acid sites, since its selectivity is rapidly decreased with the deactivation of catalyst (table 4). Both MBYNE and PRENAL are also formed in a relatively high quantity over H-ZSM-5 samples, then Brønsted acid sites are also active for the formation of MBYNE and PRENAL in MBOH reactions.

The formation of HMB was also suggested to require the presence of both acid and basic sites. However, this compound could not be detected in any significant amount in this work.

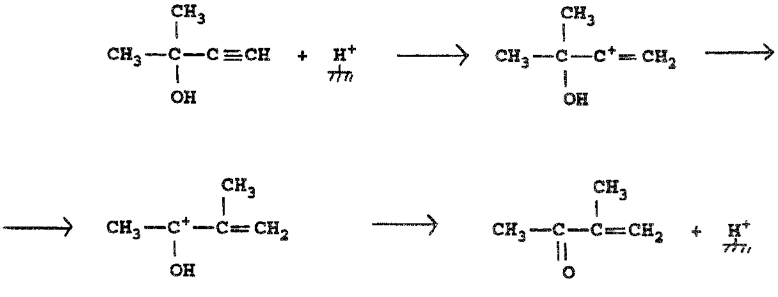

Scheme 3.

4.2. CATALYST DEACTIVATION

The deactivation with reaction time is apparently serious for all alkali-exchanged zeolites. Infrared results revealed that after reaction at 180°C not only the reactant MBOH was still adsorbed, but also the product acetone is condensed into diacetone alcohol and strongly adsorbed on alkali-exchanged X zeolites. This is certainly the reason of the carbon unbalance observed in the beginning of reaction (5 min). However, mainly in the case of X zeolites, it is found that the carbon unbalance became positive when the deactivation occurred after long time reaction (55 min). This may be explained by the reaction of previously adsorbed MBOH. The adsorption of diacetone alcohol became weak over Y and L zeolites as indicated by the weak 1420 cm^{-1} and also weak C=O bands. Thus the strong condensation and adsorption of acetone product and also the reactant (MBOH) adsorption are the main reasons for the deactivation over X zeolites, and this is also a reason for the deactivation over Y and L zeolites. It is noted that the deactivation became less important over Cs-X and Na-A samples, which have the strongest basicity and therefore weakest Lewis acidity. At first glance this is hard to understand since the strong basicity should favour the condensation of acetone, and then the deactivation should become more serious. In our opinion, in agreement with the proposal of Lewis acid sites recently suggested by Kazansky [18], the Lewis basic sites should be considered as acid–base pairs in which the neighbouring cations are also important (see schemes 1 and 2). For comparison, figs. 6a and 6b plot the change in infrared band intensity of the C=O bond ($\nu 1$) for both X and other Na-exchanged zeolites. The abscissas are the charges on oxygen and cation (divided by the square of the atomic radius), which are calculated from Sanderson's electronegativity equalization method [3,19] based on the atomic parameters recommended by Sanderson [19]. The former is an indication of zeolite base strength [3,20], while we suggest that the latter can be an approach to Lewis acid strength of the cations. Clearly, a volcano relationship can be found between the band intensity and both the Lewis acid and Lewis base strength for the open circle points, which represent the samples where diacetone alcohol was detected by infrared spectra. The highest band intensities are observed in the cases of Na- and Li-X samples, which possess suitable base and also acid strengths. Thus not only the basic site but also the alkali cation which possesses high enough acid strength are necessary for the condensation of acetone. The low Si/Al ratio in Na-A zeolite and the high electropositivity of Cs cation in Cs-X zeolite will produce a high basicity of framework oxygen but weak Lewis acidity of cations, therefore the production of diacetone alcohol will become less on Cs-X sample as confirmed by infrared band intensity, and not observed on Na-A sample, then the deactivation over these samples also becomes less important. By contrast, the condensation of acetone becomes less important over Y and L zeolites and negligible over mordenite and ZSM-5 samples due to their weak basicity. Figs. 6c and 6d further correlate the C=O vibration frequencies (both $\nu 1$ and $\nu 2$) with the base and acid strength. It is interesting to find

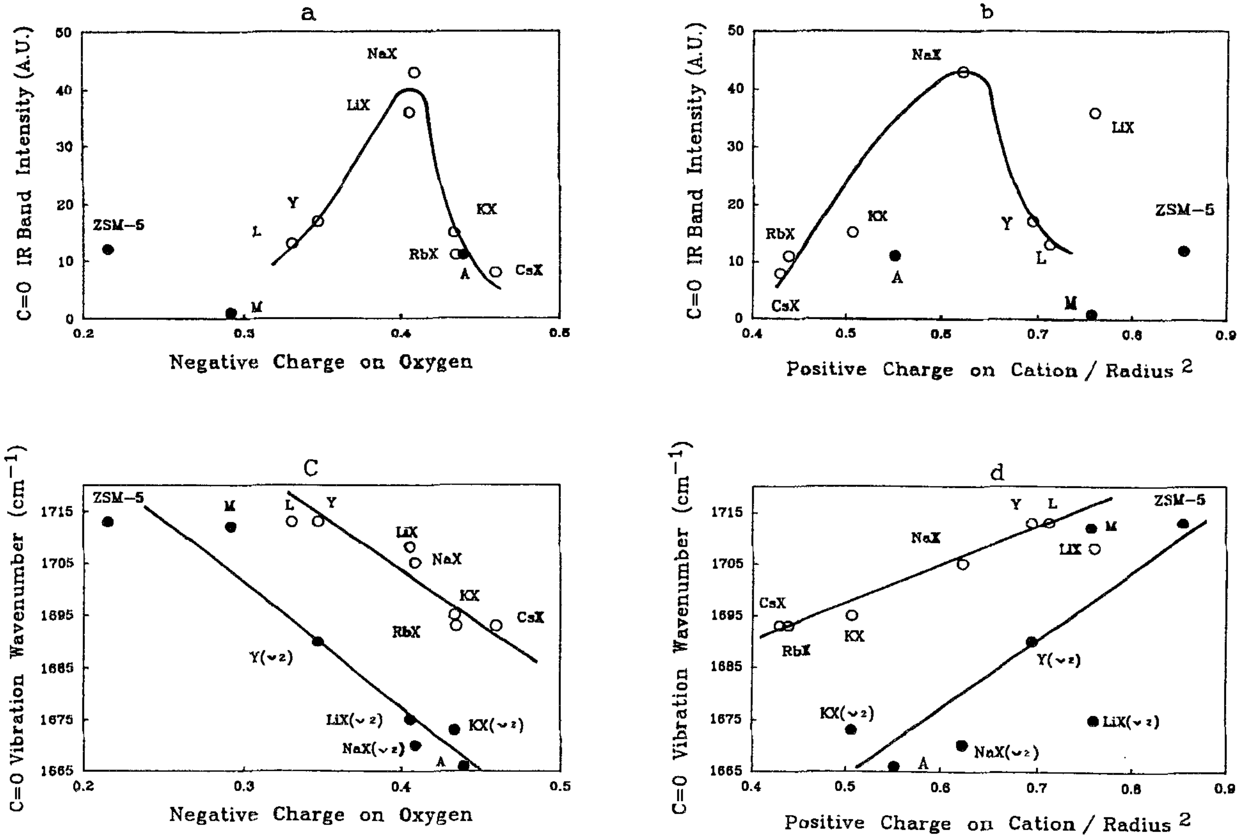

Fig. 6. Relationship between the main C=O infrared band ($\nu 1$) intensity and (a) the negative charge on framework oxygen; (b) the positive charge on cation divided by square of the atom radius. Relationship between the C=O infrared vibration frequencies ($\nu 1$ and $\nu 2$) and (c) the negative charge on framework oxygen; (d) the positive charge on cation divided by square of the atom radius. The open circles represent samples where diacetone alcohol was formed.

that the data can be divided into two groups satisfying two straight lines. The open circles represent again the samples where diacetone alcohol was formed, while there is no condensation observed over samples represented by the solid circles. Thus we concluded that the main C=O band for Na-A, mordenite and ZSM-5 samples possesses the same nature of the second C=O band observed for Li-X, Na-X, K-X and Na-Y samples, that is, the adsorbed acetone. In the case of diacetone alcohol adsorption, the most possible adsorption form could be the interaction between OH group and the cation, because the oxygen in this group should possess more negative charge than that in the C=O group. On the other hand, acetone would be directly adsorbed on cations through the oxygen of C=O group, and the adsorption should be weaker compared with alcohol. However, the correlation in fig. 6d is not very well, particularly for the point representing the Li-X sample. This may mean that the charges on cation divided by the square of the atomic radius is not a perfect description of the Lewis acid strength. In any case, the detail model of both acetone and diacetone alcohol adsorption, and therefore their dependence upon the acidity still keep unclear.

The main deactivation reason for H-ZSM-5 and alkali-exchanged ZSM-5 and mordenite then must be different. The protons are the main acid sites in H-ZSM-5, while the main sites in alkali-exchanged ZSM-5 and mordenites are also not the basic sites but the Lewis acid sites. Consequently, no bands around 2920 and 1420 cm^{-1} were found for these samples after reaction at 180°C. Instead, some weak bands around 1600 cm^{-1} can be detected. Thus, not the condensation of acetone, but the coke formation on Brønsted or Lewis acid sites could be the main reason for the deactivation over these zeolites. Consequently, it is the coke formation which caused the carbon unbalance observed over these samples. This may be the reason why no acetone was detected though a small amount of acetylene was observed over these samples. The coke formation may also be the other reason for the deactivation over zeolite L and Li-X samples, since some weak bands around 1600 cm^{-1} also appeared for these samples.

5. Conclusion

(1) The Lewis basic sites catalyze the cleavage reaction of MBOH. The product acetone easily condenses into diacetone alcohol and is strongly held by the conjugate Lewis acid sites: this is the main reason for the deactivation observed over alkali-exchanged X zeolites.

(2) The strong Lewis acid sites catalyze the dehydration of MBOH, which results in the formation of MBYNE.

(3) The catalytic conversion of MBOH to MIPK requires the presence of not Lewis acid but strong Brønsted acid sites. The Brønsted acid sites are also active for the formation of MBYNE and PRENAL in MBOH reactions. The combination

of Lewis acid and Lewis base sites is not effective for the formation of HMB in MBOH reactions.

(4) The Si/Al ratio of zeolite framework provides an easy way to tune up the relative strengths of both Lewis basic and Lewis acid sites.

References

[1] M. Huang and S. Kaliaguine, in: *Progress in Catalysis*, eds. K.J. Smith and E.C. Sanford (Elsevier, Amsterdam, 1992) p. 291.
[2] M. Huang, A. Adnot and S. Kaliaguine, J. Am. Chem. Soc., in press.
[3] M. Huang and S. Kaliaguine, J. Chem. Soc. Faraday Trans. 88 (1992) 751.
[4] M. Huang, A. Adnot and S. Kaliaguine, J. Catal., in press.
[5] H. Lauron-Pernot, F. Luck and J.M. Popa, Appl. Catal. 78 (1991) 213.
[6] R. Borade, A. Sayari, A. Adnot and S. Kaliaguine, J. Phys. Chem. 94 (1990) 5989.
[7] *The Sadtler Standard Spectra* (Sadtler Research Laboratories, Philadelphia, 1980).
[8] K. Nakanishi, *Infrared Absorption Spectroscopy* (Nankodo, Tokyo, 1962).
[9] G. Zhang, H. Hattori and K. Tanabe, Appl. Catal. 40 (1988) 183.
[10] J.W. Ward, in: *Zeolite Chemistry and Catalysis*, ACS monograph 171 (Am. Chem. Soc., Washington, 1979) p. 118.
[11] P. Pichat, J.C. Vedrine, P. Gallezot and B. Imelik, J. Catal. 32 (1974) 190.
[12] P.B. Venuto, in: *Catalysis in Organic Synthesis* (Academic Press, New York, 1977).
[13] M. Huang and S. Kaliaguine, J. Mol. Catal., in press.
[14] M. Derewinski, J. Haber and J. Ptaszynski, in: *New Developments in Zeolite Science and Technology*, Proc. 7th Int. Zeolite Conference, eds. Y. Murakami, A. Iijima and J.W. Ward (Kodansha/Elsevier, Tokyo/Amsterdam, 1986) p. 957.
[15] W.J. Mortier and R.A. Schoonheydt, Prog. Solid Stat. Chem. 16 (1985) 1.
[16] J.A. Rabo and G.J. Gajda, Catal. Rev.-Sci. Eng. 31 (1990) 385.
[17] E.D. Bergmann, J. Am. Chem. Soc. 73 (1951) 1218.
[18] V.B. Kazansky, in: *Catalysis and Adsorption by Zeolites*, eds. G.Öhlmann, H. Pfeifer and R. Fricke (Elsevier, Amsterdam, 1991) p. 117.
[19] R.T. Sanderson, *Chemical Bonds and Bond Energy* (Academic Press, New York, 1976).
[20] D. Barthomeuf, J. Phys. Chem. 88 (1984) 42.